

Article

Spatial Variability Analysis of Renewal Time in Harbour Environments Using a Lagrangian Model

Yaiza Samper^{1,*}, Ivan Hernández¹, Leidy M. Castro-Rosero^{1,2}, Maria Liste¹, Manuel Espino^{1,*}
and José M. Alsina^{1,3}

- ¹ Departament d'Enginyeria Civil i Ambiental (DECA), Laboratori d'Enginyeria Marítima (LIM), Universitat Politècnica de Catalunya-BarcelonaTech (UPC), C. Jordi Girona, 1-3, 08034 Barcelona, Spain; ivan.hernandez1@upc.edu (I.H.); lemcastroro@gmail.com (L.M.C.-R.); maria.liste@upc.edu (M.L.); jose.alsina@upc.edu (J.M.A.)
- ² Facultat de Ciències de la Terra, Universitat de Barcelona, Avinguda C. de Martí i Franquès, s/n, 08028 Barcelona, Spain
- ³ Departament d'Enginyeria Gràfica i de Disseny, Universitat Politècnica de Catalunya-BarcelonaTech (UPC), Avinguda Diagonal 647, 08034 Barcelona, Spain
- * Correspondence: yaiza.julia.samper@upc.edu (Y.S.); manuel.espino@upc.edu (M.E.)

Abstract: The water quality in port domains is highly dependent on the capacity for renewal and mixing with external water. This study uses Lagrangian modelling to investigate renewal time in Barcelona, Tarragona, and Gijón harbours (Spain), which represent semi-enclosed micro-tidal and meso-tidal environments. For this purpose, different particle-tracking simulations have been carried out in each of the ports to study the trends of circulation and water renewal trends both on the surface layer and at the bottom. The results indicate that in microtidal Mediterranean ports, the renewal time is longer at the bottom (32 days in Barcelona and 61 days in Tarragona). Conversely, in the mesotidal port of Gijón, located on the Cantabrian coast, the opposite pattern is observed, with higher renewal times at the surface (14 days). While the results from Lagrangian modelling exhibit magnitudes comparable to in situ measurements from previous studies, it remains essential to evaluate the specific characteristics of each method and compare these findings with other similar works.

Keywords: water renewal time; numerical modelling; Lagrangian model; harbours; water quality



Academic Editors: Nuno Vaz, Ryan J.K. Dunn and Ana Picado

Received: 10 January 2025

Revised: 3 February 2025

Accepted: 11 February 2025

Published: 13 February 2025

Citation: Samper, Y.; Hernández, I.; Castro-Rosero, L.M.; Liste, M.; Espino, M.; Alsina, J.M. Spatial Variability Analysis of Renewal Time in Harbour Environments Using a Lagrangian Model. *J. Mar. Sci. Eng.* **2025**, *13*, 341. <https://doi.org/10.3390/jmse13020341>

Copyright: © 2025 by the authors. Licensee MDPI, Basel, Switzerland. This article is an open access article distributed under the terms and conditions of the Creative Commons Attribution (CC BY) license (<https://creativecommons.org/licenses/by/4.0/>).

1. Introduction

Ports play a crucial role as industrial and economic hubs, while also having various impacts on their surrounding areas. Their activity generates environmental pressure on their physical surroundings, having a negative impact on air, water, and soil quality [1]. Ports are often situated near urban centres and there is a growing trend to exploit these areas for recreational, tourist, and nautical activities [2]. This highlights the need to assess and manage the environmental impacts stemming from port activities [3,4]. Coastal regions near ports are highly vulnerable to pollution, which impacts their resources and activities. Water circulation in these areas significantly influences the residence time of pollutants and, therefore, the water quality in harbours.

Circulation patterns at the regional coastal scale are influenced by different factors such as waves, tides, wind, larger-scale currents, etc. [5] and have been studied over time using different methodologies. However, as the scale and intensity of these forcings are decreased, hydrodynamic characterization becomes more complex, as in estuaries or

harbours [6], where transport and mixing processes are typically less intense due to their semi-enclosed nature [7]. In these spaces, the renewal capacity depends mainly on the water exchange fluxes between the interior and the exterior, in addition to the internal circulation itself [8]. In the case of harbours, their compartmentalized geometry further divides water movements. Therefore, it is important to study the spatial variation in water renewal time (RT) within these domains. RT is a key indicator of water quality in harbours and is defined as the average time a water particle remains within the harbour area [9]. This offers a primary description of the multiple processes involved in transport and serves as a key parameter in controlling system behaviour [10].

This spatial variability has been analysed in different contexts and using different methodologies [11] to calculate and analyse the renewal time in the Pontevedra estuary using a stationary box model. Stamou et al. (2007) [12] proposed a methodology to calculate the water renewal time in semi-enclosed coastal areas with complex geometries, using the hydrodynamic model FLOW-3D. In this case, modelling is employed to illustrate future circulation and renewal conditions of water in response to the necessity of carrying out significant dredging. The authors emphasized the importance of wind and tides in the variability of renewal times. Orfila et al. (2005) [13] investigated the renewal times in the port of Cabrera Island using measured data from an ADCP, comparing them with simulations of a continuous stirred tank reactor (CSTR) model. Grifoll et al. (2013) [14] characterized the water renewal locally in Bilbao Harbour by a Eulerian model, highlighting its spatial variation both horizontally and vertically. The most commonly used tool for this analysis is numerical modelling because there are insufficient or inadequate campaign data for these calculations [15,16]. Another example of work that uses Eulerian models to study the renewal time of a semi-confined water mass is by Dias et al. (2000) [17] who examined the residence time of a bay using a particle-tracking model that calculates particle positions at each time step.

In this study, the renewal time in the ports of Barcelona, Tarragona, and Gijón is characterized using a Lagrangian particle-tracking model (LPTM). These ports differ in key aspects. Barcelona and Tarragona are situated in microtidal environments typical of the Mediterranean coast, while Gijón is located in a mesotidal environment along the Cantabrian coast. Additionally, the port of Barcelona has two mouths, unlike the single-mouth structures of Tarragona and Gijón. Previous studies [18,19] estimated the integrated RT of each port using current data from the port entrances collected during intensive measurement campaigns, yielding time series data of daily mean RT values for each harbour.

The main objective of this study is to calculate and analyse the spatial distribution of RT at various depths within each harbour. Unlike previous research, which generally focused on calculating RT as a single integrated value for entire ports or bays [20], this work provides both an integrated RT value and a spatially resolved, depth-specific analysis. This approach enables us to examine RT variations across different zones and depths, addressing a significant gap in locally specific and depth-resolved RT data. Such detailed analysis offers new insights into water renewal dynamics and local water quality variations within harbour environments, contributing a level of understanding that previous studies have not achieved.

The tool used in this study is the LOCATE model [21], which simulates the release of Lagrangian particles over the entire extension of the harbours. Through different simulations and post-processing techniques, the renewal time on the surface layer and at the bottom in the whole domain of the three mentioned ports has been estimated, by spatially integrated and specific areas.

This article is structured into five main sections: firstly, it presents the context on which this study is based; next, it describes the ports, the model configuration, and the methodology for calculating the renewal time; thirdly, it analyses the results; fourthly, it presents a discussion comparing these results with those obtained in previous studies, with different hypotheses and reasoning; and finally, the conclusions of this study are presented.

2. Materials and Methods

2.1. Study Area

The ports examined in this study are situated at different locations along the Spanish coast. Barcelona and Tarragona are located in the northeast of the peninsula, along the Mediterranean Sea, while Gijón is situated in the north, facing the Cantabrian Sea (Figure 1). The general characteristics of each of them are described below. The measurement campaigns referenced throughout the article, as well as the methodology used to calculate renewal times from the measurements at the mouths, are detailed in Samper et al. (2023 and 2022) [18,19].

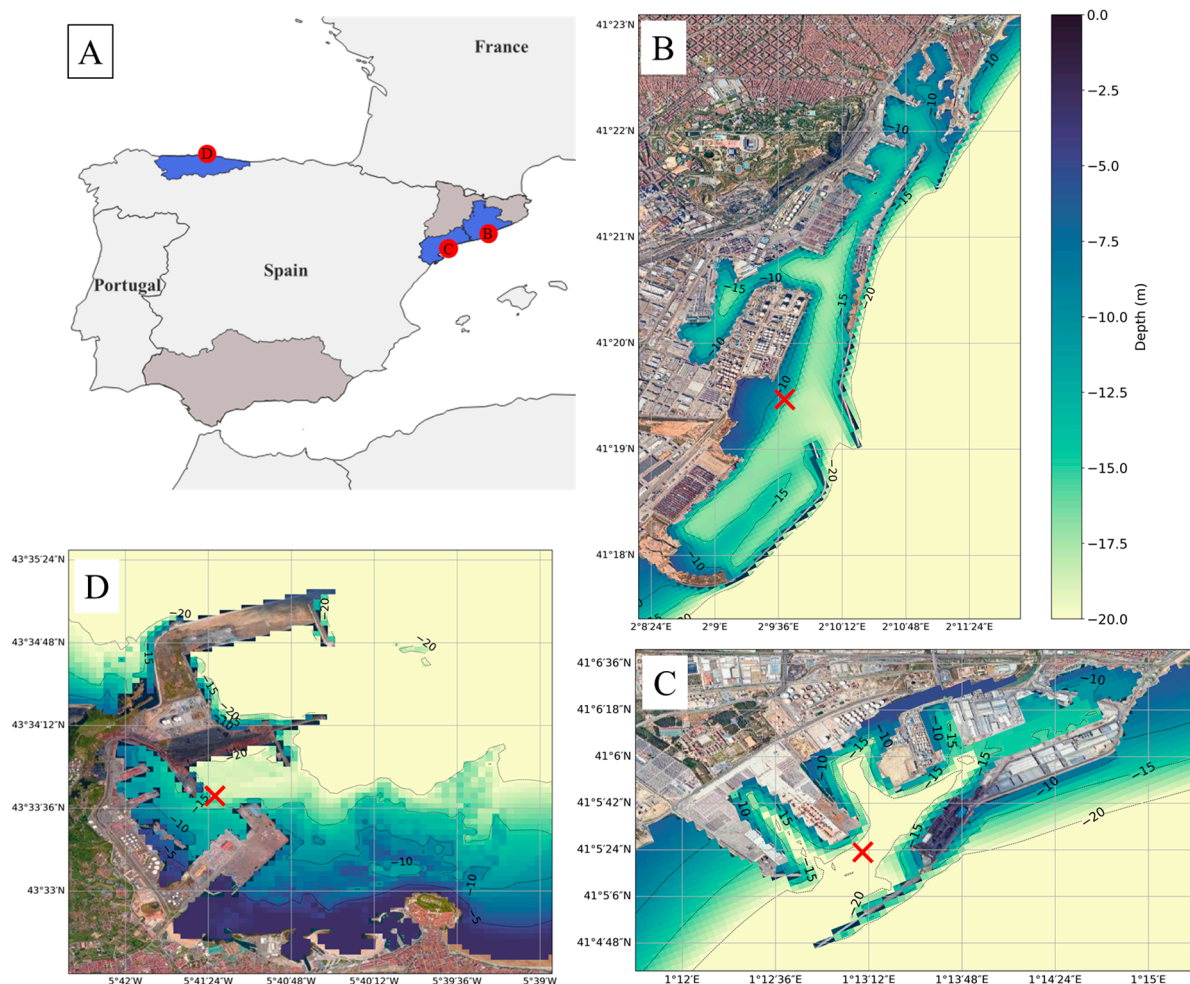


Figure 1. Location (A) and bathymetric maps of the ports of Barcelona (B), Tarragona (C), and Gijón (D). The red crosses indicate the locations of the ADCP Doppler devices during the measurement campaigns referenced earlier, used for validation and calculations in previous studies.

2.1.1. Barcelona Harbour

The port of Barcelona is located on the Catalan coast, on the Mediterranean Sea. It is approximately 10 km long and up to 2 km wide, with a longitudinal axis oriented 30° clockwise from north. It connects with the open sea through two mouths: one on the

north and the other on the south, measuring 145 and 530 m wide, respectively. This port features a complex geometry characterized by several channels and basins of different shapes and sizes with depths ranging from 8 to 20 m [22] (Figure 1B). Internal currents are strongly influenced by coastal currents and wind, which in winter conditions have been described as negative estuarine circulation [23]. In previous work [18], the average renewal time of the harbour was estimated to be 18 days from current measurements at the southern entrance.

2.1.2. Tarragona Harbour

The port of Tarragona is situated on the southern coast of Catalonia covering approximately 4 km in length and between 200 m and 1 km in width. It has a longitudinal axis oriented to the northeast and depths ranging between 10 and 20 m [24] (Figure 1C). The Francolí River flows into the interior, with a significant seasonal variation in flow, with an average monthly summer flow (recorded 6 km upstream from the port) of $0.2 \text{ m}^3/\text{s}$, which increases to $1.4 \text{ m}^3/\text{s}$ in winter [25]. The port is connected to the sea by a 570-m-wide mouth, situated in the southern section of the harbour. According to other studies [18], based on observations, the average renewal time is estimated to be 11 days.

2.1.3. Gijón Harbour

The port of Gijón is located in the south of the Bay of Biscay, in the northern part of the Iberian Peninsula. It has natural protection against the characteristic north-westerly storms because it is safeguarded by the cape of Peñas y Torres and the Amouscas platform [26]. The marine circulation in this region is complex, characterized by seasonal currents that vary in strength and direction and are significantly influenced by the Gulf Stream and marine topography [27,28]. The bathymetry of the inner harbour reveals depths ranging from 5 to 20 m (Figure 1D) and the tidal range can reach 4.36 m [29]. Previous studies have estimated the average water renewal time to be 21 days, with an increase in renewal time observed under high atmospheric pressure conditions [19].

2.2. Model and Hydrodynamic Description

The main tool used in this study is LOCATE v.1.0, a numerical model that integrates Eulerian hydrodynamic data from the SAMOA system (Sistema de Apoyo Meteorológico y Oceanográfico a las Autoridades Portuarias) with Lagrangian particle simulations using Parcels (Probably a Really Efficient Lagrangian Simulator) [30]. Parcels is a particle Lagrangian solver that allows customized simulations using different tools in Python 3 [31]. The scripts used and instructions for their use are described in the LOCATE repository on Github by Hernández et al. (2024) [21].

The hydrodynamic information has been obtained from the high-resolution numerical models implemented in SAMOA, which uses the ROMS (Regional Ocean Modelling System) hydrodynamic model [32]. Numerical details, complete data, and source code are available on the ROMS website, <https://www.myroms.org/> (accessed on 10 February 2024). SAMOA (main features in Table 1) has been developed by Puertos del Estado (PdE), the Maritime Engineering Laboratory of the Polytechnic University of Catalonia (LIM-UPC), and different Spanish port authorities and responds to the need for meteorological and oceanographic information at coastal and port levels [33]. This model was selected for its high resolution, enabling analysis at very small scales such as harbours, as well as for its accessibility and ease of access to information. The hydrodynamic data utilized in this study can be found in the PdE data catalogue: <https://opendap.puertos.es> (accessed on 10 February 2024). This model has two regular nested grids with a horizontal spatial resolution of 350 m for the coastal domains and 70 m for the port domains. The vertical resolution comprises 20 and 15 levels, respectively [34].

Table 1. Main features of SAMOA computational domains.

| Harbour | Domain | Dimension (Cells) | Extension (Km) |
|-----------|---------|-------------------|-----------------|
| Barcelona | Coastal | 170×72 | 64×27 |
| | Harbour | 165×153 | 12×11 |
| Tarragona | Coastal | 260×166 | 100×65 |
| | Harbour | 130×125 | 9×9 |
| Gijón | Coastal | 223×115 | 78×40 |
| | Harbour | 222×142 | 15×10 |

The operational SAMOA system is nested in the regional daily forecasts provided by CMEMS-IBI (Copernicus Marine Environment Monitoring Service-Iberia Biscay Irish). On the one hand, CMEMS-IBI provides hourly current and sea level data, which are utilized as open boundary conditions (OBC). Additionally, it supplies daily temperature and salinity values throughout the water column. In cases of significant freshwater discharge, river discharge is factored in, considering climatological data and maintaining a constant salinity of 18 PSU. On the other hand, SAMOA at the surface is influenced by wind stress with hourly frequency, along with atmospheric pressure, water fluxes (evaporation), and surface heat provided by the Agencia Estatal de Meteorología (AEMET). AEMET's data is derived from the HARMIONE model (2.5 km resolution nested within the IFS forecast of the ECMWF) [35]. To ensure sufficiently detailed bathymetry, global data sources such as GEBCO <https://www.gebco.net/> (accessed on 10 February 2024) and local data provided by port authorities are combined. Extended information on the SAMOA model is available at Álvarez et al. (2018) and Sotillo et al. (2019) [33,36].

SAMOA has been successfully validated through multiple approaches, including comparison with alternative models [34], measurements [33], and under different scenarios [37]. The current model results are validated at the mouth by comparing the observations with the simulations (see Figure 1 for the validated measurement locations). This validation is divided into two phases: a first visual representation of the time series and a second analysis by calculating the correlation coefficient (R) and the root-mean-square error (RMSE) [38]. Figure 2 shows the time series of simulated and measured currents during the different campaigns and the statistics calculated corresponding to each case and the corresponding scatter plot.

The qualitative analysis demonstrates that the SAMOA model captures the overall pattern observed in the different ports, reflecting the temporal evolution of currents reasonably well. However, some discrepancies are observed in terms of intensity. Specifically, in the port of Gijón, the model slightly underpredicts the current intensity, particularly during periods of higher flow rates. Conversely, in the ports of Barcelona and Tarragona, the model tends to overpredict the current intensity.

Despite these differences, the model consistently reproduces the directional patterns of the currents, distinguishing periods of inward and outward flows with notable accuracy. This alignment with the observed patterns supports the model's applicability for general trend analysis, even though localized intensity variations require further refinement.

The studies that we referenced have successfully validated the model in external areas, particularly near the coast, where currents are stronger and more predictable. This external validation is robust and reliable, and, given that the internal currents within the harbour are closely linked to these external currents, we consider this to support the model's applicability within the harbour as well. However, validation within the harbour area presents greater challenges due to the much lower current intensities and the complex geometry of the port [39].

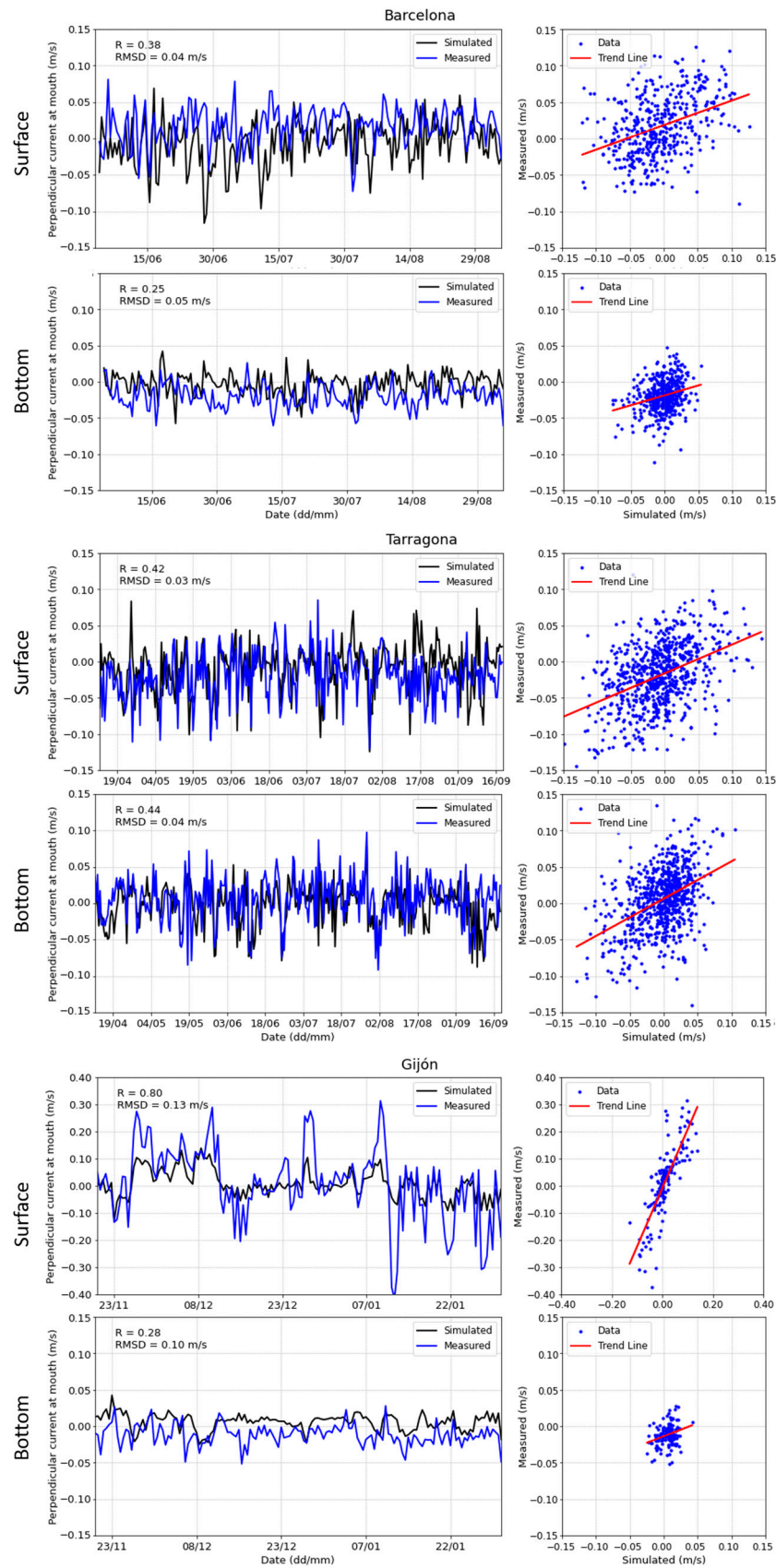


Figure 2. Time series and scatter plots of current intensity in the direction perpendicular to the harbour entrance, at the surface and at the bottom. Positive values indicate currents flowing inward, while negative values represent currents flowing outward. Observations are represented by blue lines, and SAMOA predictions are shown in black.

The statistical results reveal correlations of 0.38, 0.42, and 0.80 at the surface, and 0.25, 0.44, and 0.28 at the bottom for Barcelona, Tarragona, and Gijón, respectively. It is important to note that both the measurements and the model predictions are influenced by the complexity of each domain, the port infrastructures, and the intensity of tides, particularly in the case of Gijón. Although the correlation coefficients between model results and observations are relatively low in some cases, they capture the observed trends. Although the correlations within the harbour are lower, we regard this initial validation as a valuable first step, and we accept these results while acknowledging the need for further investigation to better understand the reasons behind these lower correlations.

2.3. Model Setup

According to the methodology from the LOCATE model proposed by Hernández et al. (2024) [21], the scripts have been adapted to the ports of Barcelona, Tarragona, and Gijón. Specifically, the adaptation was applied to a preprocessing script containing the particle release information, which is adjusted based on the port being analysed. For each of these ports, two simulations are conducted (surface and bottom), with the duration of each simulation defined according to the duration of the measurement campaigns mentioned in the previous work (Table 2).

Table 2. Key simulation parameters: number of nodes, particles, and duration of the simulations.

| Harbour | Nodes Inside Harbour | Number of Simulated Particles | Simulation Duration (Days) |
|-----------|-------------------------|----------------------------------|-------------------------------|
| Barcelona | 1514 | 1514 | 90 |
| Tarragona | 765 | 1530 | 152 |
| Gijón | 587 | 1174 | 73 |

The transport processes considered in the movement of particles include coastal currents, turbulent diffusion, and the specific boundary conditions of each port. The availability of high-resolution data for different coastlines has allowed for the application of boundary conditions that accurately represent the complex geometry of the ports. To achieve this, a pre-calculated distance grid between the nodes of the hydrodynamic model and the high-resolution coastline is utilized. This approach enables the precise identification of particles near the contours of the harbours, allowing them to be returned to their immediate previous positions. This process enables particles to ‘bounce’ and continue circulating.

The model simulates the movement of discrete particles that are passively moving due to currents, providing a trajectory for each particle. The simulations of the trajectories are started at a specific time (corresponding to the beginning of the measurement campaigns of the previous work) along the entire inland water mass of the ports and have different durations to coincide with the duration of the measurement campaigns [18,19]. A pre-processing step, which combines tools from Python and the open-source software QGIS 3.30.3, is used to extract the coordinates of the SAMOA hydrodynamic grid nodes inside each port. Subsequently, particles are placed on these nodes. For Barcelona, one particle is placed at each node (Figure 3A), while for Tarragona and Gijón, two particles are situated at each node. This ensures that all simulations have a minimum of 1000 particles. Table 2 summarizes the values of these parameters for each port.

The definition of the simulated diffusive phenomenon (K_h) depends on factors such as mesh size, resolution, and current intensity [40]. However, experimental data are not easily available to define its value for the scale used and for each of the analysed ports.

To determine the most consistent value in the simulations, validation has been conducted using data from a drifting buoy in the port of Barcelona.

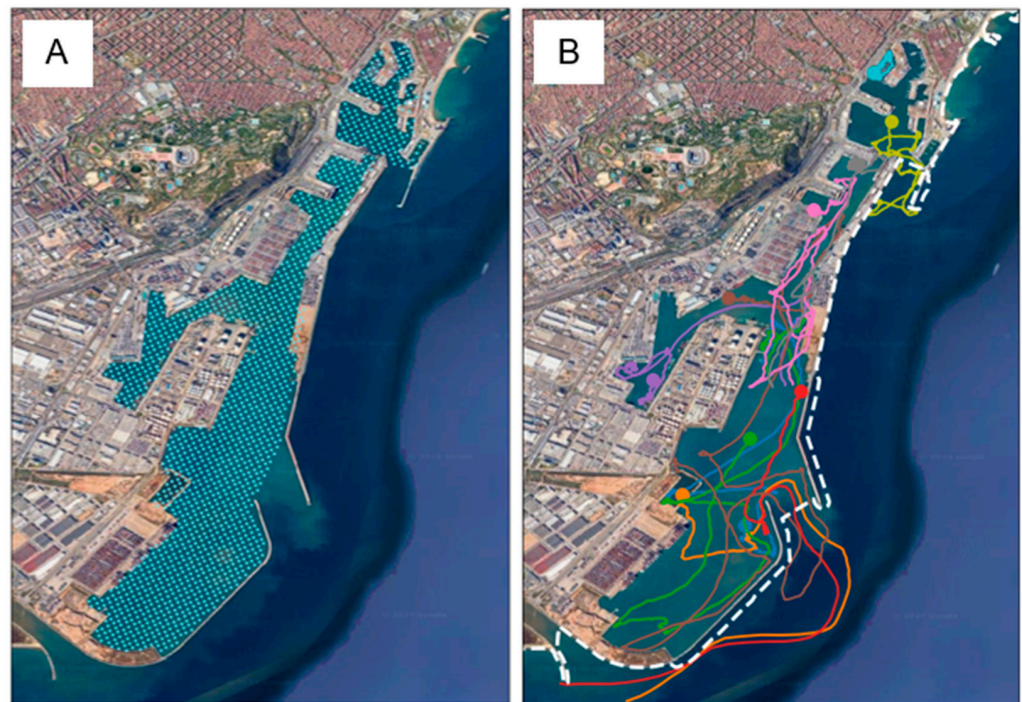


Figure 3. Example of the location of the particle launching nodes in the port of Barcelona (A). Simulation of trajectories for 10 particles within the port of Barcelona during one week. Initial locations are represented by points, trajectories are represented by solid lines, and the dashed white line marks the point from where it is considered to be outside the port (B).

Using observational data (Figure 4), trajectories of five simulated particles with different K_h values have been compared with the observed trajectory of the buoy. The Normalized Cumulative Lagrangian Separation (NCLS) distance Skill Score (SS) methodology proposed by Liu and Weisberg (2011) [41], previously utilized with this model by Castro-Rosero et al. (2023) [42] and Hernández et al. (2024) [21], was applied. The NCLS quantifies the fit of the simulated trajectories to the real ones, with lower values indicating more accurate simulations. The SS is calculated from cumulative values over all time steps using a tolerance threshold ‘ n ’, as proposed by Liu and Weisberg (2011) [41] and Révelard et al. (2021) [43]. In this case, the tolerance threshold ‘ n ’ has been set to 16, taking into account that the SS is quantified in a range from 0 to 1, where an SS of 1 implies an exact match between the simulated and observed trajectories, indicating a high level of accuracy in the simulation [44]. To carry out these calculations, the Python module `geopy.distance` was used, using the WGS-84 ellipsoid as the geodetic reference, as specified in the 2022 Geopy documentation [45].

In this case, the constant horizontal diffusion coefficient with the highest SS is $0.05 \text{ m}^2 \text{ s}^{-1}$ (Figure 4), which is the value used in all simulations. Between $0.01 \text{ m}^2 / \text{s}$ and $0.05 \text{ m}^2 / \text{s}$, the SS shows small variation but it was observed that above $0.05 \text{ m}^2 \text{ s}^{-1}$, the SS increased and the model performance decreased. Although 0.1 may appear closer to the real trajectory due to its proximity, the simulation with $K_h 0.05 \text{ m}^2 / \text{s}$ aligns better because of its straighter shape. Similar coefficients have also been used in problems of similar geometric dimensions to ours [36,37].

Regarding the validation of the Lagrangian trajectories and the diffusion coefficient, it is important to note that such coefficients are typically not extensively validated in the literature, largely due to the limited studies available on this topic [46]. In our study,

however, we sought to validate our approach by using a buoy in the port of Barcelona as a small-scale example. The results that we obtained were consistent with the limited data available in the literature, which led us to consider this validation satisfactory for our purposes.

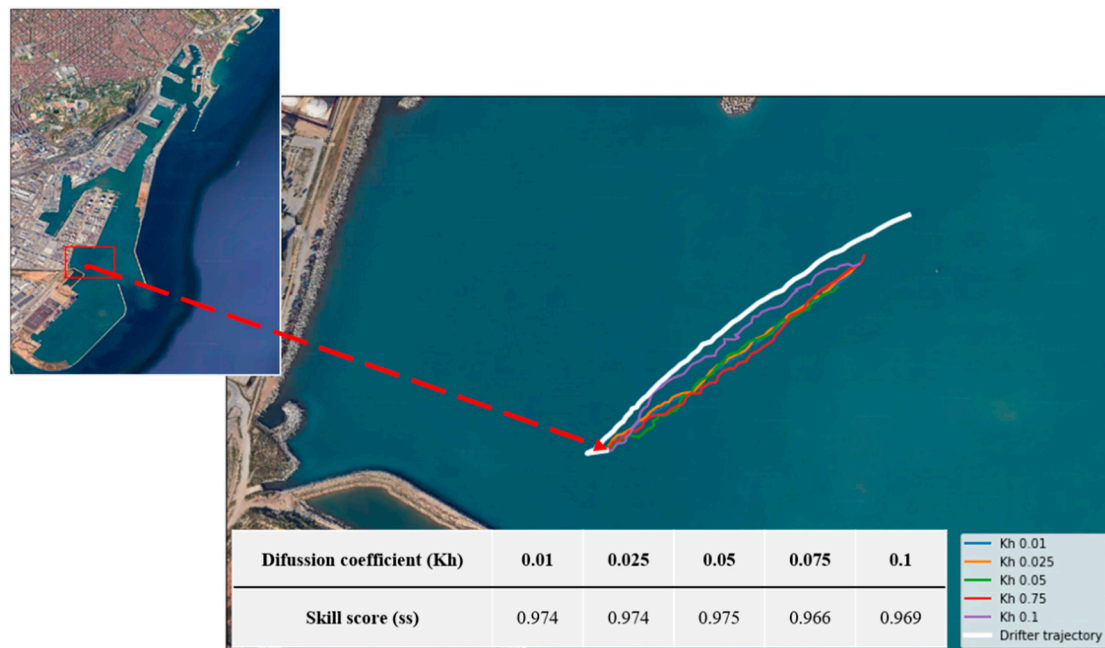


Figure 4. Recorded trajectory (white line) and simulated trajectories with different horizontal diffusion coefficients (K_h) in the port of Barcelona.

2.4. Renewal Times

To calculate the renewal time, the moment at which each particle leaves the port was identified and compared with the simulation start time. To determine that a particle is outside, two polygons were created and differentiated using the shapely library in Python [47]: one representing the water mass within the port and the other representing the water outside (see Figure 3B). Using the geopy library ‘geopy’ (2022) [44], which facilitates the manipulation and analysis of geometric elements and enables work with geo-referenced information, particle coordinates at each time step were obtained. For computational efficiency, data were recorded at 15 min intervals.

To spatially analyse the simulation results, each port has been subdivided into different zones based on prominent features such as separate docks, breakwaters, or other constructions dividing the water body (Figure 5). In addition, it has been tried to maintain a similar number of zones for all of them. This allows a geospatial analysis to identify areas with the highest susceptibility to pollution problems. In addition, these areas have been defined to facilitate comparison with the results obtained in previous studies.

As mentioned in Section 2.3 (Model Setup), the duration of each simulation corresponds to the duration of the measured campaigns in previous work, allowing a direct comparison of the results. During the simulations, not all particles leave the port. Those particles remaining inside at the end of the simulation are assigned a renewal time equal to the full duration: 90 days for Barcelona, 152 days for Tarragona, and 73 days for Gijón. Once renewal times are assigned to each particle, integrated calculations and statistical analyses are conducted both overall and by zones.

To enhance the clarity and reproducibility of our research methodology, we have developed a flowchart (Figure 6) that outlines the key processes and analytical steps undertaken throughout this study. This visual representation serves not only to address

feedback regarding the methodology's accessibility for individuals unfamiliar with the software utilized but also to provide a comprehensive overview of our approach. By illustrating the sequential stages of analysis, the flowchart facilitates a better understanding of the underlying processes and allows for easier replication of our results by other researchers. This structured approach ensures that critical information regarding input data and methodological descriptions is readily available, fostering greater transparency in our scientific contributions.

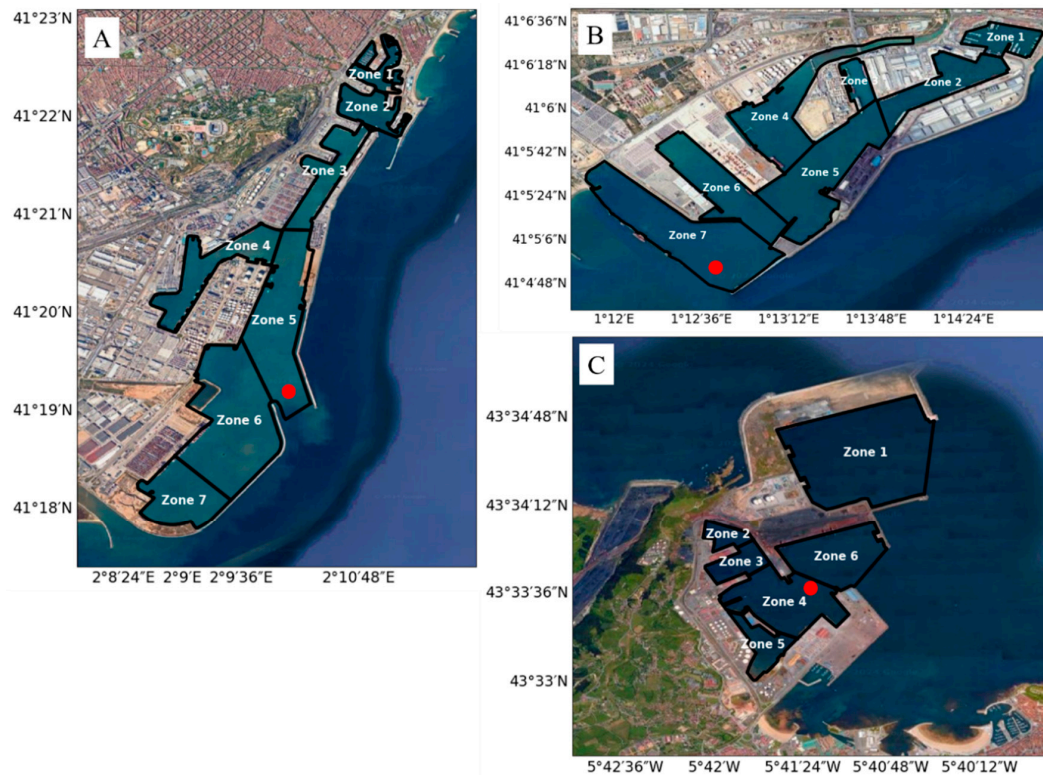


Figure 5. Delimitation of the areas considered in the ports of Barcelona (A), Tarragona (B), and Gijón (C). The red dots represent the reference points used later for the current profile analysis.

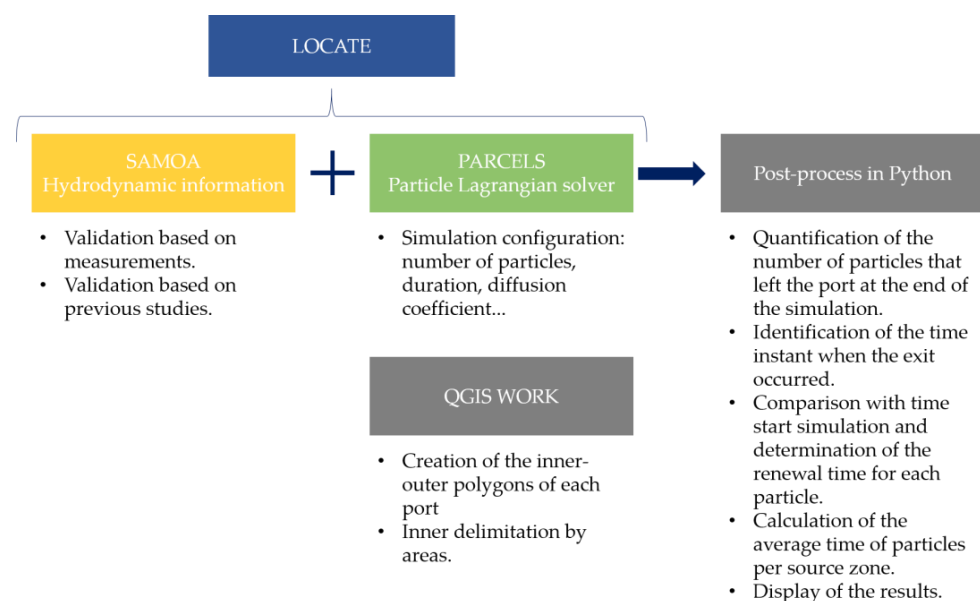


Figure 6. A flowchart detailing the key stages of analysis and methodology used in this study, aimed at providing clarity for reproducibility and understanding of the processes involved.

3. Results

This section presents the results of the numerical experiments carried out in the different ports. In each case, the analysis includes both the surface and bottom levels, showing different behaviours between the two simulations. The obtained results vary not only vertically, but also with their horizontal position. In addition to the spatial distribution maps of the renewal times, tables also show the results in terms of days and the percentage of particles that, by the end of the simulation, have either left each zone or remained in the interior.

3.1. Barcelona Harbour

Figure 7 shows the spatial distribution of the renewal time within the port of Barcelona, calculated from the trajectories of 1514 particles over the entire length of the port in a 90-day simulation. Surface values vary from 11 days in areas near the harbour mouths to 44 days in points furthest from the exterior. At deeper waters, although the spatial distribution pattern is the same (longer renewal time in sheltered areas), more extreme figures are obtained, ranging from 5 to 86 days. Regarding the integrated value of the entire port, an average renewal time of 21 days at the surface and 32 days at the bottom is estimated. Generally, higher renewal times are observed at the bottom, except in zones 6 and 7, which differ from this pattern.

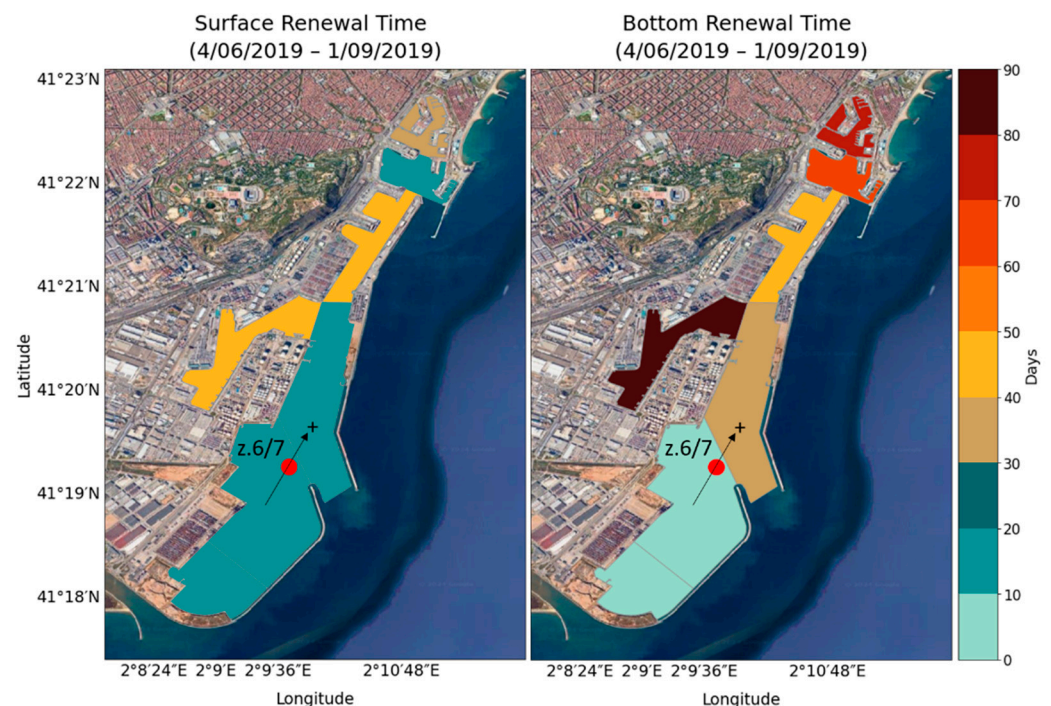


Figure 7. Spatial distribution of the mean renewal time in the port of Barcelona for the period 4 June 2019–1 September 2019, calculated from the surface (**left**) and bottom (**right**) simulated particle trajectories. The red dot indicates the location of the profile analysed in the discussion.

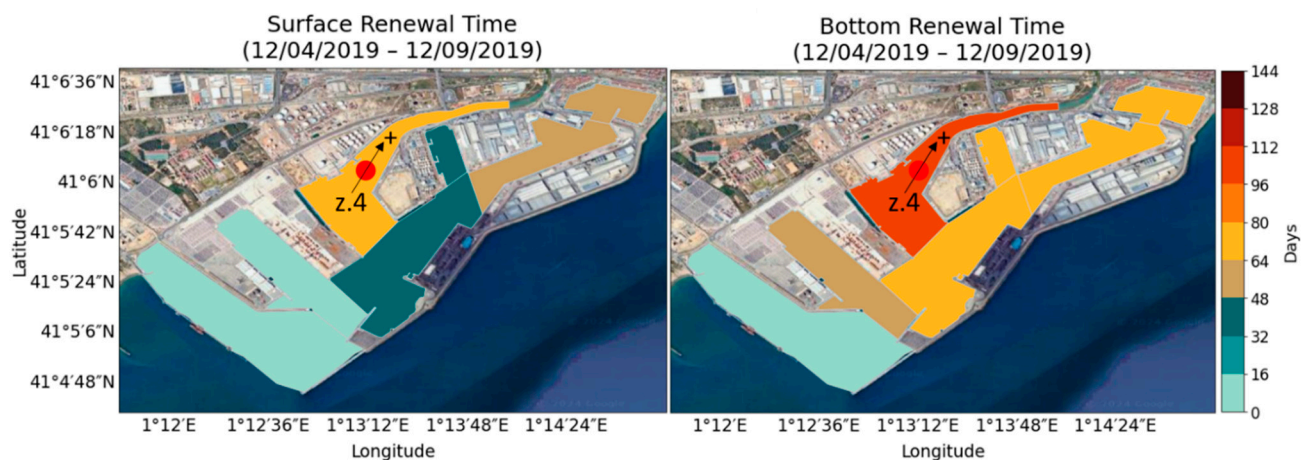
At the end of the simulation, 9.8% of the surface particles and 26.9% at the bottom (Table 3) remained within the interior of the port, so they are assigned a renewal time of 90 days, equivalent to the simulation duration. In all of the zones, at least 70% of the particles are exported at the surface and 8% at the bottom. Significant differences between the surface and bottom are observed in zone 4, where 79.0% and 8.7% are exported respectively, and where the average renewal time is higher.

Table 3. Statistical results of the renewal time by zones in the port of Barcelona for the period from 4 June 2019–1 September 2019.

| Zone | Particle Number | Exported Particles (%) | | Non-Exported Particles (%) | | Mean RT (Days) | |
|----------------|-----------------|------------------------|--------|----------------------------|--------|----------------|--------|
| | | Surface | Bottom | Surface | Bottom | Surface | Bottom |
| 1 | 72 | 70.8 | 38.9 | 29.2 | 61.1 | 38.7 | 70.4 |
| 2 | 91 | 91.2 | 48.3 | 8.8 | 51.7 | 17.4 | 60.3 |
| 3 | 142 | 75.4 | 64.6 | 24.6 | 35.4 | 44.4 | 45.6 |
| 4 | 195 | 79.0 | 8.7 | 21.0 | 91.3 | 42.4 | 85.7 |
| 5 | 321 | 94.4 | 72.9 | 5.6 | 27.1 | 11.1 | 37.6 |
| 6 | 502 | 95.0 | 99.6 | 5.0 | 0.4 | 13.8 | 4.8 |
| 7 | 191 | 99.5 | 100 | 0.5 | - | 12.0 | 4.7 |
| Total/ Mean | 1514 | 90.2 | 73.1 | 9.8 | 26.9 | 21.0 | 32.4 |

3.2. Tarragona Harbour

The results of the Tarragona simulations are shown in Figure 8. This simulation has a duration of 152 days, the longest in this study, and includes 1530 particles. Similar to previous cases, the estimated renewal times at the surface are lower than those at the bottom. Surface renewal times range from 3 to 65 days, while bottom renewal times range from 10 to 111 days, depending on proximity to the port mouth. Integrated results for the entire harbour give a renewal time of 36 days at the surface and 61 days at the bottom.

**Figure 8.** Spatial distribution of the mean renewal time in the port of Tarragona for the period 12 April 2019–15 September 2019, calculated from the surface (**left**) and bottom (**right**) simulated particle trajectories. The red dot indicates the location of the profile analysed in the discussion, while the arrow represents the orientation of the positive direction of the vector.

The 19.5% of particles at the surface and 23% at the bottom (Table 4) that have not been exported at the end of the simulation time are assigned a renewal time of 152 days, equivalent to the simulation duration. Analysing these results by zone, it is observed that at the surface, a minimum of 59.9% of particles are exported from all zones, while at the bottom 36.3% of all zones are exported. There are no significant differences between the surface and the bottom, but there are substantial differences between the different zones. In the case of zone 4, low percentages of exported particles are observed, particularly at the bottom. An integrated renewal time of 88 days is estimated for this zone, considering both surface and bottom layers.

Table 4. Statistical results of the renewal time by zones in the port of Tarragona for the period from 4 June 2019–1 September 2019.

| Zone | Particle Number | Exported Particles (%) | | Non-Exported Particles (%) | | Mean RT (Days) | |
|----------------|-----------------|------------------------|--------|----------------------------|--------|----------------|--------|
| | | Surface | Bottom | Surface | Bottom | Surface | Bottom |
| 1 | 86 | 76.7 | 89.5 | 23.3 | 10.5 | 61.5 | 64.3 |
| 2 | 190 | 67.9 | 88.4 | 32.1 | 11.6 | 61.8 | 64.7 |
| 3 | 50 | 74.0 | 82.0 | 26.0 | 18.0 | 46.3 | 71.3 |
| 4 | 322 | 59.9 | 36.3 | 40.1 | 63.7 | 65.4 | 110.8 |
| 5 | 326 | 79.5 | 76.4 | 20.5 | 23.6 | 37.8 | 69.0 |
| 6 | 228 | 97.8 | 89.9 | 2.2 | 10.1 | 7.3 | 48.3 |
| 7 | 328 | 99.1 | 97.9 | 0.9 | 2.1 | 2.5 | 10.1 |
| Total/ Mean | 1530 | 80.5 | 77.0 | 19.5 | 23.0 | 36.1 | 61.4 |

3.3. Gijón Harbour

The results for Gijón (Figure 9) are based on the simulation of the trajectory of 1174 particles over 73 days. In this case, a different spatial distribution of renewal times is observed compared to the previous ports. The results at the surface range from 2 to 39 days, while those at the bottom range from 2 to 11. Notably, higher values are observed at the surface than at the bottom, with the exception of zone 1, which corresponds to an independent part of the harbour with its own mouth. The results also vary according to their proximity to the outside of the port, with higher values observed in the more sheltered areas and farther away from the mouth of the harbour. Estimation renovation time averages for this port were 14 days on the surface and 5 days on the bottom.

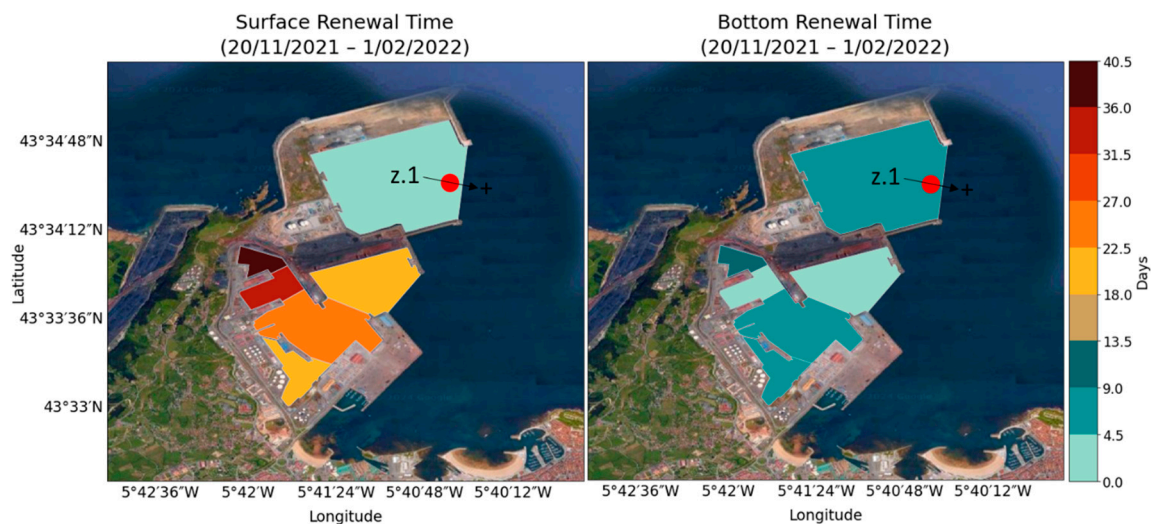


Figure 9. Spatial distribution of the mean renewal time in the port of Gijón for the period 20 November 2021–1 February 2022, calculated from the surface (**left**) and bottom (**right**) simulated particle trajectories. The red dot indicates the location of the profile analysed in the discussion, while the arrow represents the orientation of the positive direction of the vector.

In the end, 6% of surface particles and 2.4% of deep particles (Table 5) remain in the interior of the port, thus giving them a renewal time of 73 days, equivalent to the simulation duration. In all zones, a minimum of 70% of the surface particles and 90% of the bottom particles are exported, with similar values between the surface and the bottom. The zone with the greatest difference is zone 2, which exports the least particles and has the longest average renewal time (25 days).

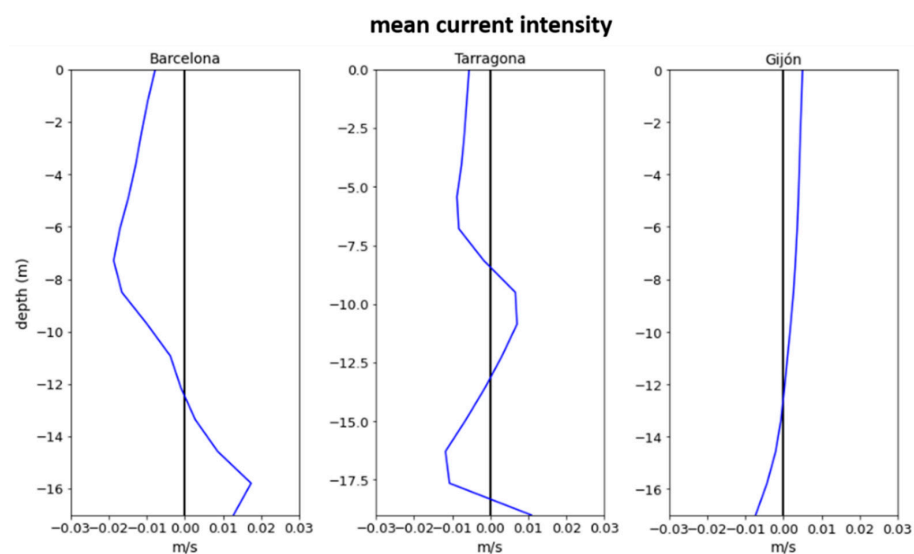
Table 5. Statistical results of the renewal time by zones in the port of Gijón for the period from 20 November 2021 to 1 February 2022.

| Zone | Particle Number | Exported Particles (%) | | Non-Exported Particles (%) | | Mean RT (Days) | |
|----------------|-----------------|------------------------|--------|----------------------------|--------|----------------|--------|
| | | Surface | Bottom | Surface | Bottom | Surface | Bottom |
| 1 | 558 | 98.9 | 98.8 | 1.01 | 1.2 | 1.7 | 5.8 |
| 2 | 40 | 70.0 | 90.0 | 30.0 | 10.0 | 39.4 | 10.7 |
| 3 | 62 | 87.1 | 100.0 | 12.9 | - | 31.9 | 2.8 |
| 4 | 256 | 88.2 | 95.1 | 11.8 | 4.9 | 25.9 | 4.9 |
| 5 | 74 | 93.2 | 96.0 | 6.8 | 4.0 | 19.4 | 4.8 |
| 6 | 194 | 94.9 | 99.0 | 5.1 | 1.0 | 20.0 | 1.7 |
| Total/ Mean | 1174 | 94.0 | 97.6 | 6 | 2.4 | 13.8 | 4.9 |

4. Discussion

In previous works, renewal times in these ports were calculated using a Eulerian approximation, involving measurements at a single point over a period of time. Samper et al. (2023, 2022) [18,19] estimated renewal times by measuring currents at the harbour mouths with a current meter and considering total water volumes. This method provided integrated values for each harbour, varying over time. In this study, however, a numerical approach is used, employing a Lagrangian numerical model that provides detailed and individualized trajectories for each simulated particle, enabling global averaging of results or analysis on a zonal scale. The following sections analyse and compare the specificities of the results obtained with those from previous works.

The results reveal varying renewal times influenced by both the initial horizontal and vertical positions of particles. As previously mentioned, Barcelona and Tarragona (two Mediterranean microtidal harbours) show higher renewal times at the bottom, whereas the opposite trend is observed in Gijón (example of mesotidal harbour). Figure 10 presents the vertical profiles of currents at the mouth of each port, where positive values indicate inflow into the port and negative values indicate outflow. The hydrodynamics represented by these profiles coincide with the results described, with inflow currents at the bottom in the first two cases and surface currents in the last one, which would generate these higher renewal times. The location of these profiles is presented in Figure 5.

**Figure 10.** Current profile at the mouth for each port during the simulated period.

Figures 11–13 present horizontal mean flow maps for each port over the entire study period, providing the mean flow data that support the renewal time results obtained in this study. These maps illustrate the weaker currents at depth compared to those at the surface, aligning with the findings of higher renewal times in deeper layers in the ports of Tarragona and Barcelona. This pattern suggests that the reduced flow intensity at the bottom likely contributes to slower water renewal in these layers, while surface currents facilitate a faster renewal rate.

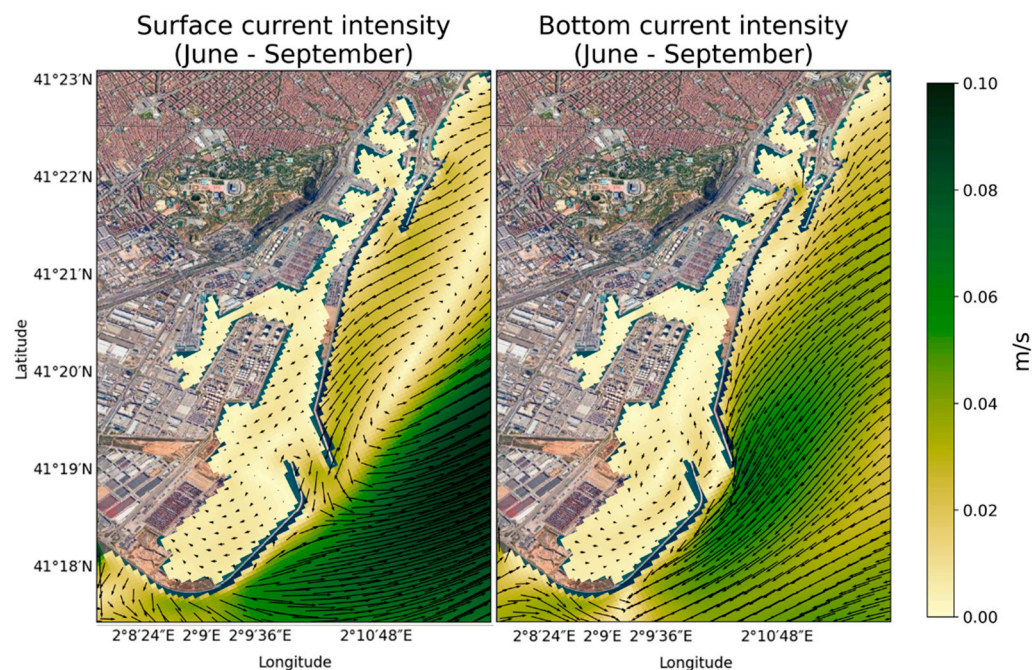


Figure 11. Maps of horizontal mean flow at the surface and bottom from June to September in Barcelona harbour. The surface currents flow out of the harbour, while the bottom currents flow inward. This pattern aligns with the current profiles shown in Figures 9 and 11, as well as with the renewal time results described.

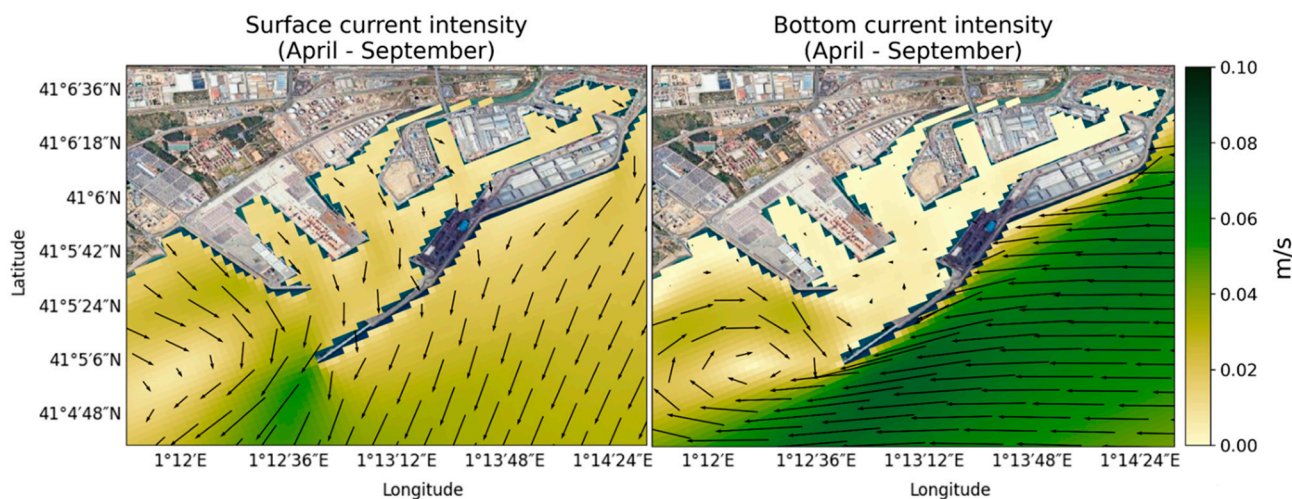


Figure 12. Maps of horizontal mean flow at the surface and bottom from April to September in Tarragona harbour. The surface currents flow out of the harbour, while the bottom currents flow inward. This pattern aligns with the current profiles shown in Figures 9 and 11, as well as with the renewal time results described.

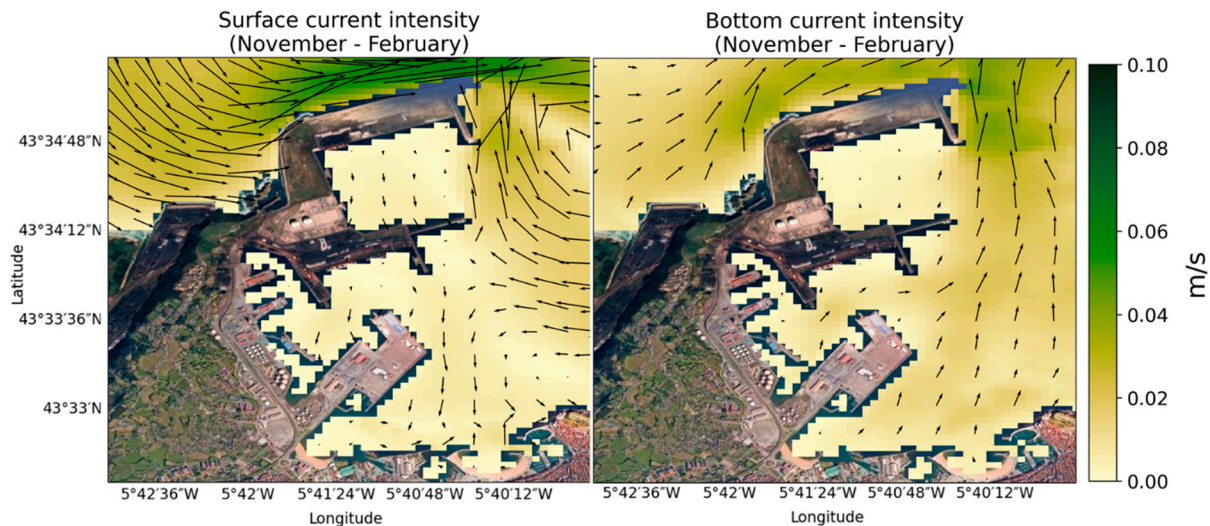


Figure 13. Maps of horizontal mean flow at the surface and bottom from November to February in Gijón harbour. The surface currents flow into the interior of the harbour, while the bottom currents flow outward. This pattern aligns with the current profiles shown in Figures 9 and 11, as well as with the renewal time results described.

In the southern basin of Barcelona, encompassing defined zones 6 and 7, a contrasting pattern is observed compared to the rest of the port, characterized by higher surface renewal times. The current profile at the mouth of the basin (Figure 14A) shows surface currents towards the interior of the basin (negative values), resulting in increased particle travel distance and, consequently, higher renewal times. The location of this profile is identified in Figure 7, where zone 4 is the one with the highest values, a greater difference between the surface (43 days) and the bottom (86 days) and also with respect to the other zones of the port. This 1.10 km² basin is connected to the main channel of the harbour but is situated away from either of the two harbour mouths. With a minimum width of 220 m, the basin features more confined waters, less intense currents, and consequently, higher RT.

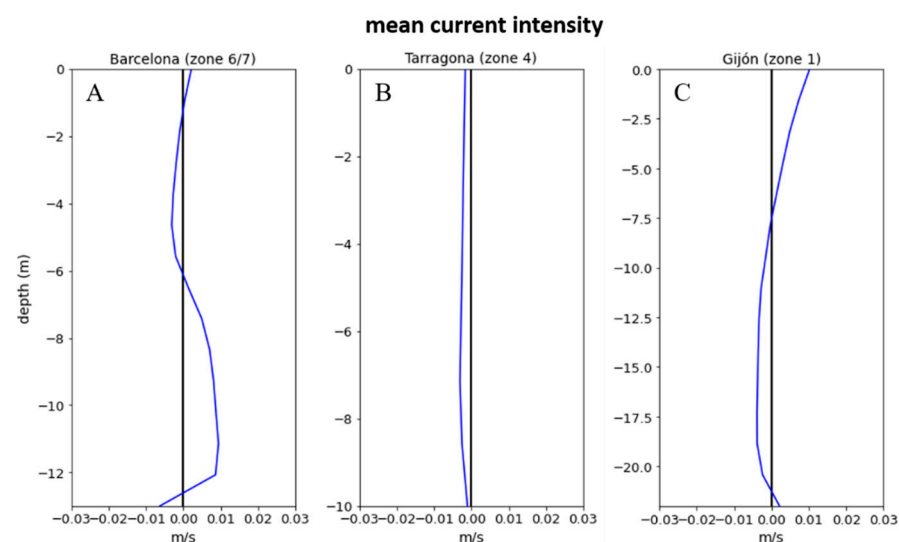


Figure 14. Current profile of areas with different patterns or where extreme results have been identified in Barcelona (A), Tarragona (B) and Gijón (C).

The results obtained in this work present an integrated mean renewal time for the entire port of 26.7 days compared to the 18 days estimated from the Doppler-measured data presented in Samper et al. (2022) [18]. These higher values include the entire harbour

domain, even the values in the most sheltered basins. In contrast, the time calculated from observations only considers data obtained at a point close to the harbour mouth and is consequently expected to be lower.

In the case of Tarragona, the same pattern is observed throughout the port domain (lower renewal times on the surface). However, zone 4 reaches values much higher than the total average for the port (65.4 days on the surface and 110.8 days on the bottom). The mouth of the Francolí River, situated within this zone, exhibits a narrow geometry ranging between 70 and 300 m. This constrained configuration impedes the easy exit of particles circulating within the zone, consequently prolonging the renewal time. The profile in Figure 14B, which corresponds to the river mouth (exact location in Figure 8) shows very-low intensity currents.

The mean integrated renewal time obtained in this study is 48.8 days, higher than that calculated in the previous studies (11 days in Samper et al. (2022) [18]). This difference may have two main causes. Firstly, as in the case of Barcelona, the calculation of the mean time from the model results includes the entire length of the harbour, covering sheltered regions characterized by lower currents. Secondly, the SAMOA hydrodynamic model incorporates a statistically predetermined flow for the Francolí River. Consequently, fluctuations such as floods or increases in river flow are not considered in the model hydrodynamics of the harbour. In the case of the results obtained from measurements at the mouth of the harbour, they may be affected by changes in river flow. The primary objective of this study is to achieve a spatial analysis of water renewal times within ports.

Therefore, even though the model may not provide highly precise correlations, it does offer a qualitative understanding of which areas or ports may face greater challenges in water renewal. Furthermore, as mentioned earlier, the model operates as an established system and has been extensively validated in other studies. It is important to highlight that the hydrodynamic model used in this study is part of the operational SAMOA system, which is managed by Puertos del Estado and not by our institution (LIM/UPC). As a result, modifications to the numerical grid, bathymetry, forcing agents, or numerical schemes cannot be implemented. Nevertheless, despite limitations in correlation with in situ observations, the model remains a valuable tool for the qualitative assessment of water exchange processes in the analysed ports.

In this context, it is important to highlight that the observed subprediction of current intensity at the port of Gijón, as well as the overprediction in Barcelona and Tarragona, could impact the numerical estimation of the RT when derived from the Lagrangian simulation. These deviations in current intensity directly influence the calculated RT. Nonetheless, the model's capability to provide spatial distributions and to distinguish zones with differing susceptibility to pollution or accumulation of residues remains unaffected.

Specifically, while numerical discrepancies in the intensity of currents may introduce uncertainties in absolute RT values, the spatial patterns identified by the model are consistent with observed trends. This enables the effective identification of areas within the ports that are more vulnerable to reduced water renewal or prone to the accumulation of contaminants. Such insights are crucial for environmental management and planning, even if the exact RT values have inherent limitations due to the model's performance at specific locations. It is important to recognize that the accuracy of the model results could be improved if certain modifications were implemented, such as refining the simulation grid, updating the bathymetry, and optimizing the forcing agents. These enhancements would likely improve correlation with in situ measurements and provide greater reliability in quantifying renewal times. However, since the SAMOA model is an external operational system, these modifications cannot be implemented within the scope of this study.

In the port of Gijón, generally higher renewal times are observed on the surface with the exception of zone 1, where the opposite is the case. Moreover, in this zone, the results obtained are considerably lower than in the rest (1.7 days on the surface and 5.8 days on the bottom). The profile in Figure 14C, situated at the basin mouth, reveals surface currents flowing outward (positive values) and weaker currents inward (negative values). This section of the harbour operates independently from the rest, directly connecting to the sea. As a result, it exhibits a lower renewal time compared to the other harbour areas. The integrated average renewal time is calculated from zones 2, 3, 4, and 5 only (see Figure 5C). This is due to the location of the current meter-Doppler in the campaign of previous works, because zones 1 and 6 were outside the domain considered for the calculation. To compare the results of this work with those obtained previously, the mean time of the zones equivalent to those considered in Samper et al. (2023) [19] was calculated, with the mean renewal time obtained in this work being 17.5 days, compared to the 21 days previously estimated. The result obtained from the numerical simulations is slightly lower than that calculated from the Doppler data at the mouth.

In Barcelona and Tarragona, a similar distribution of renewal times is observed, with higher values at the bottom and in the most sheltered areas. However, even though the port of Barcelona is considerably larger, it has lower renewal times. This may be due to the existence of two harbour entrances, one in the north and the other in the south, which facilitates the circulation of particles towards the outside of the port and, therefore, reduces the renewal time. Orfila et al. (2005) [13] estimated the renewal time in a Mediterranean port (Cabrera) by simulating the release of Lagrangian particles and calculating the time elapsed from their release until they exit the port. This study, which employs a similar methodology to the current research, reveals that renewal times are higher at the bottom compared to those at the surface, aligning with our findings.

Gijón, however, has the opposite vertical disposition of the renewal times, meaning that the highest renewal times are observed on the surface. This distinction can be attributed to the port's location on the Cantabrian coast, characterized by significantly stronger tides, exceeding 4 m, compared to the Mediterranean Sea [48]. Consequently, these tides create inward and outward currents in deeper layers generating water exchange between the port and the external environment, thus reducing renewal times. The same vertical distribution of renewal time (higher at the surface) was observed in Bilbao, another Cantabrian environment, in Grifoll et al. (2013) [14], attributed to the effect of sea breezes countering the influence of tides in deeper layers.

This current configuration at the harbour entrances, particularly in the Mediterranean ports, resembles positive estuarine circulation in the form of a salt-wedge. In this type of circulation, freshwater from a river or surface runoff meets denser seawater, creating a wedge-like structure where the less saline, fresher water flows out towards the exterior at the surface, while denser saltwater flows in at depth [49]. This results in a net outflow of water at the surface, which contributes to lower renewal times in the Mediterranean harbours. In contrast, Gijón, with its mesotidal environment, exhibits characteristics of a partially mixed negative estuary (without freshwater input from the harbour) [50,51]. Here, tidal forces lead to more uniform mixing, producing a more even distribution of currents and influencing the renewal time patterns differently.

Regarding the horizontal distribution of renewal times, in all three ports, it is observed that the most sheltered areas or those farther from the harbour mouths experience greater difficulty renewing the water within them [52]. This pattern emphasizes the need for special attention to these areas, particularly in the case of pollution events, as reduced water exchange could exacerbate the persistence of contaminants [53]. Local conditions, such as the specific geometry of each port, the degree of confinement, and hydrodynamic features,

play a crucial role in shaping renewal patterns. For instance, sheltered regions with narrow passages or complex bathymetry often exhibit weaker circulation, which contributes to longer renewal times [54]. These findings underscore the importance of considering local hydrodynamic characteristics when assessing water quality and management strategies in port environments.

For future research, it would be beneficial to assess the impact of changes in horizontal resolution in specific port areas, the inclusion of forcing factors with improved spatial and temporal resolution, and the optimization of numerical parameters associated with advective and diffusion processes. These adjustments could enhance the correlation between modelled results and observations, providing a more precise characterization of water renewal processes in port environments.

5. Conclusions

The spatial distribution of water renewal time in various harbours was characterized using a Lagrangian simulation model of particle trajectories. This approach allows tracking the horizontal movement of particles across the water body, providing a detailed and specific overview of water renewal in different areas of the harbour. Moreover, it accounts for the influence of local topography and morphological factors, providing a better understanding of hydrodynamics of the harbour.

The results from this study were compared with those obtained in our previous studies where this parameter was estimated using a Eulerian approach, specifically based on measurements at single points at the harbour mouths. While Eulerian measurements offer an integrated perspective on the average renewal time for the entire harbour, it may underestimate it due to its inability to consider the harbour's morphological complexity.

The comparison reveals similarities between both methods in terms of magnitude, although with differences that need to be considered. The analysis reveals that in Mediterranean ports such as Barcelona and Tarragona, the renewal time is higher at the bottom, whereas in Gijón, situated in the Cantabrian Sea, it is higher at the surface. The presence of intense tides probably facilitates the exchange of water between the interior and exterior of the port at the bottom, coupled with the strong influence of the breeze at the surface. Additionally, higher renewal times have been identified in sheltered areas or areas far from the harbour mouths in all cases.

The methodology utilized in this study enabled a precise visualization of areas within harbours that are most susceptible to contamination or spillage issues, facilitating the design of targeted prevention and intervention plans in the event of potential accidents. By employing a Lagrangian numerical approach, this study goes beyond the scope of traditional Eulerian methods, allowing a detailed analysis of renewal times across distinct spatial scales—surface, bottom, and defined zones within each port. This contributes a new layer of understanding to the field, providing specific insights into the dynamics of water renewal that can be especially relevant in semi-enclosed and sheltered port areas, where water exchange is naturally more limited.

However, the limitations of this method in comparison to other approaches must be considered. While Lagrangian modelling provides detailed spatial insights, it relies heavily on high-resolution hydrodynamic data, which, though increasingly available, is not yet universally accessible for all port locations. Additionally, there are inherent constraints in the hydrodynamic model itself, such as the exclusion of real-time river flow data. For ports situated near rivers, fluctuations in river discharge can significantly influence local hydrodynamics, impacting water renewal times and spatial flow patterns. This factor is particularly relevant in ports like Tarragona, where such influences could alter the predicted renewal times. Another limitation stems from the duration of each simulation: particles

remaining within the port at the end of the simulation period are assigned a renewal time equal to the simulation's duration. This cap may skew the average results slightly lower than actual renewal times in ports with longer retention periods. Additionally, it should be noted that the renewal times estimated in this study are based on specific seasonal conditions from the months of data collection; therefore, variations in weather or season may lead to changes in these seasonal results.

Despite these limitations, this approach offers a detailed, nuanced spatial view of port hydrodynamics, assessing the vulnerability of port ecosystems without necessitating direct measurements from current meters or weather stations. This characteristic enhances its potential utility for environmental management, especially in ports where monitoring resources may be limited. Through an innovative adaptation of the LOCATE Lagrangian numerical model—originally developed for marine debris tracking—this study demonstrates its applicability in analysing temporal hydrodynamic parameters at any depth within harbour environments. This flexibility and adaptability highlight the model's potential for a broader range of applications, positioning it as a valuable tool in the scientific and practical advancement of harbour water quality and management strategies.

Author Contributions: Conceptualization, Y.S. and M.E.; Methodology, Y.S., I.H., L.M.C.-R., M.L., M.E. and J.M.A.; Validation, L.M.C.-R.; Formal analysis, Y.S. and J.M.A.; Investigation, Y.S., I.H., M.L. and M.E.; Writing—original draft, Y.S.; Writing—review & editing, Y.S., I.H., L.M.C.-R., M.L., M.E. and J.M.A.; Supervision, M.L. and M.E. All authors have read and agreed to the published version of the manuscript.

Funding: This work was supported by Eco-Bays R&D project PID2020-115924RB-I00, funded by MCIN/AEI/10.13039/501100011033 and Banco Santander grant.

Institutional Review Board Statement: Not applicable.

Informed Consent Statement: Not applicable.

Data Availability Statement: Data are contained within the article.

Conflicts of Interest: The authors declare no conflict of interest.

References

1. Gupta, A.K.; Gupta, S.K.; Patil, R.S. Environmental Management Plan for Port and Harbour Projects. *Clean Technol. Environ. Policy* **2005**, *7*, 133–141. [\[CrossRef\]](#)
2. Daamen, T.A.; Vries, I. Governing the European Port–City Interface: Institutional Impacts on Spatial Projects between City and Port. *J. Transp. Geogr.* **2013**, *27*, 4–13. [\[CrossRef\]](#)
3. Wenning, R.J.; Della Sala, S.; Magar, V. Role of risk assessment in environmental security planning and decision-making. In *Environmental Security in Harbors and Coastal Areas*; Linkov, I., Kiker, G.A., Wenning, R.J., Eds.; NATO Security through Science Series; Springer: Dordrecht, The Netherlands, 2007; pp. 329–341. ISBN 978-1-4020-5800-4.
4. Dinwoodie, J.; Tuck, S.; Knowles, H.; Benhin, J.; Sansom, M. Sustainable Development of Maritime Operations in Ports. *Bus. Strategy Environ.* **2012**, *21*, 111–126. [\[CrossRef\]](#)
5. Wong, L.A.; Chen, J.C.; Xue, H.; Dong, L.X.; Su, J.L.; Heinke, G. A Model Study of the Circulation in the Pearl River Estuary (PRE) and Its Adjacent Coastal Waters: 1. Simulations and Comparison with Observations. *J. Geophys. Res.* **2003**, *108*, 2002JC001451. [\[CrossRef\]](#)
6. Cucco, A.; Umgiesser, G. Modeling the Venice Lagoon Residence Time. *Ecol. Model.* **2006**, *193*, 34–51. [\[CrossRef\]](#)
7. Mestres, M.; Sierra, J.P.; Sánchez-Arcilla, A. Factors Influencing the Spreading of a Low-Discharge River Plume. *Cont. Shelf Res.* **2007**, *27*, 2116–2134. [\[CrossRef\]](#)
8. Umgiesser, G.; Ferrarin, C.; Cucco, A.; De Pascalis, F.; Bellafiore, D.; Ghezzi, M.; Bajo, M. Comparative Hydrodynamics of 10 Mediterranean Lagoons by Means of Numerical Modeling. *J. Geophys. Res. Ocean.* **2014**, *119*, 2212–2226. [\[CrossRef\]](#)
9. Lettmaa, A. OFFICER, C.B. 1976. Physical Oceanography of Estuaries (and Associated Coastal Waters). John Wiley and Sons, Inc., New York, Xii + 465 p. \$27.50. *Limnol. Oceanogr.* **1977**, *22*, 975–976. [\[CrossRef\]](#)
10. Rueda, F.J.; Cowen, E.A. Exchange between a Freshwater Embayment and a Large Lake through a Long, Shallow Channel. *Limnol. Oceanogr.* **2005**, *50*, 169–183. [\[CrossRef\]](#)

11. Gómez-Gesteira, M.; de Castro, M.; Prego, R. Dependence of the Water Residence Time in Ria of Pontevedra (NW Spain) on the Seawater Inflow and the River Discharge. *Estuar. Coast. Shelf Sci.* **2003**, *58*, 567–573. [\[CrossRef\]](#)
12. Stamou, A.I.; Memos, C.; Spanoudaki, K. Estimating Water Renewal Time in Semi-Enclosed Coastal Areas of Complicated Geometry Using a Hydrodynamic Model. *J. Coast. Res.* **2007**, *50*, 282–286. [\[CrossRef\]](#)
13. Orfila, A.; Jordi, A.; Basterretxea, G.; Vizoso, G.; Marbà, N.; Duarte, C.M.; Werner, F.E.; Tintoré, J. Residence Time and Posidonia Oceanica in Cabrera Archipelago National Park, Spain. *Cont. Shelf Res.* **2005**, *25*, 1339–1352. [\[CrossRef\]](#)
14. Grifoll, M.; Del Campo, A.; Espino, M.; Mader, J.; González, M.; Borja, Á. Water Renewal and Risk Assessment of Water Pollution in Semi-Enclosed Domains: Application to Bilbao Harbour (Bay of Biscay). *J. Mar. Syst.* **2013**, *109–110*, S241–S251. [\[CrossRef\]](#)
15. Braunschweig, F.; Martins, F.; Chambel, P.; Neves, R. A Methodology to Estimate Renewal Time Scales in Estuaries: The Tagus Estuary Case. *Ocean Dyn.* **2003**, *53*, 137–145. [\[CrossRef\]](#)
16. Darbra, R.M.; Pittam, N.; Royston, K.A.; Darbra, J.P.; Journee, H. Survey on Environmental Monitoring Requirements of European Ports. *J. Environ. Manag.* **2009**, *90*, 1396–1403. [\[CrossRef\]](#)
17. Dias, J.M.; Lopes, J.E.; Dekeyser, I. Lagrangian Transport of Particles in Ria de Aveiro Lagoon, Portugal. *Phys. Chem. Earth Part B Hydrol. Ocean. Atmos.* **2001**, *26*, 721–727. [\[CrossRef\]](#)
18. Samper, Y.; Liste, M.; Mestres, M.; Espino, M.; Sánchez-Arcilla, A.; Sospedra, J.; González-Marco, D.; Ruiz, M.I.; Álvarez Fanjul, E. Water Exchanges in Mediterranean Microtidal Harbours. *Water* **2022**, *14*, 2012. [\[CrossRef\]](#)
19. Samper, Y.; Espino, M.; Liste, M.; Mestres, M.; Alsina, J.M.; Sánchez-Arcilla, A. Study of Atmospheric Forcing Influence on Harbour Water Renewal. *Water* **2023**, *15*, 1813. [\[CrossRef\]](#)
20. Monsen, N.E.; Cloern, J.E.; Lucas, L.V.; Monismith, S.G. A Comment on the Use of Flushing Time, Residence Time, and Age as Transport Time Scales. *Limnol. Oceanogr.* **2002**, *47*, 1545–1553. [\[CrossRef\]](#)
21. Hernández, I.; Castro-Rosero, L.M.; Espino, M.; Torrent, J.M.A. LOCATE v1.0: Numerical Modelling of Floating Marine Debris Dispersion in Coastal Regions Using Parcels v2.4.2. *Geosci. Model Dev.* **2024**, *17*, 2221–2245. [\[CrossRef\]](#)
22. Galea, A.; Grifoll, M.; Roman, F.; Mestres, M.; Armenio, V.; Sanchez-Arcilla, A.; Zammit Mangion, L. Numerical Simulation of Water Mixing and Renewals in the Barcelona Harbour Area: The Winter Season. *Environ. Fluid Mech.* **2014**, *14*, 1405–1425. [\[CrossRef\]](#)
23. Autoridad Portuaria de Barcelona Memoria Anual de Sostenibilidad de Puerto de Barcelona. Available online: <https://www.portdebarcelona.cat/es/conoce-el-puerto/autoridad-portuaria/memorias-anuales> (accessed on 10 February 2024).
24. Sánchez-Arcilla, A.; González-Marco, D.; Bolaños, R. A Review of Wave Climate and Prediction along the Spanish Mediterranean Coast. *Nat. Hazards Earth Syst. Sci.* **2008**, *8*, 1217–1228. [\[CrossRef\]](#)
25. Mestres, M.; Pau Sierra, J.; Sánchez-Arcilla, A. Baroclinic and Wind-Induced Circulation in Tarragona Harbour (Northeastern Spain). *Sci. Mar.* **2007**, *71*, 223–238. [\[CrossRef\]](#)
26. González-Marco, D.; Sierra, J.P.; Fernández de Ybarra, O.; Sánchez-Arcilla, A. Implications of Long Waves in Harbor Management: The Gijón Port Case Study. *Ocean Coast. Manag.* **2008**, *51*, 180–201. [\[CrossRef\]](#)
27. Borja, A.; Collins, M. *Oceanography and Marine Environment of the Basque Country*; Elsevier Oceanography Series; Elsevier: Amsterdam, The Netherlands, 2004; Volume 70, ISBN 978-0-444-51581-0.
28. Rubio, A.; Solabarrieta, L.; Gonzalez, M.; Mader, J.; Castanedo, S.; Medina, R.; Charria, G.; Aranda, J.A. Surface Circulation and Lagrangian Transport in the SE Bay of Biscay from HF Radar Data. In Proceedings of the 2013 MTS/IEEE OCEANS, Bergen, Norway, 10–14 June 2013; pp. 1–7.
29. Autoridad Portuaria de Gijón. *Memoria AP Gijón 2020*; APJ: Gijón, Spain, 2020; p. 146.
30. Delandmeter, P.; Van Sebille, E. The Parcels v2.0 Lagrangian Framework: New Field Interpolation Schemes. *Geosci. Model Dev.* **2019**, *12*, 3571–3584. [\[CrossRef\]](#)
31. Van Sebille, E.; Kehl, C.; Lange, M.; Delandmeter, P.; The Parcels Contributors. *Parcels*, v2.4.2; Zenodo: Geneva, Switzerland, 2023. [\[CrossRef\]](#)
32. Shchepetkin, A.F.; McWilliams, J.C. The Regional Oceanic Modeling System (ROMS): A Split-Explicit, Free-Surface, Topography-Following-Coordinate Oceanic Model. *Ocean Model.* **2005**, *9*, 347–404. [\[CrossRef\]](#)
33. Sotillo, M.; Cerralbo, P.; Lorente, P.; Grifoll, M.; Espino, M.; Sánchez-Arcilla, A.; Álvarez-Fanjul, E. Coastal Ocean Forecasting in Spanish Ports: The SAMOA Operational Service. *J. Oper. Oceanogr.* **2019**, *13*, 37–54. [\[CrossRef\]](#)
34. García-León, M.; Sotillo, M.G.; Mestres, M.; Espino, M.; Fanjul, E.Á. Improving Operational Ocean Models for the Spanish Port Authorities: Assessment of the SAMOA Coastal Forecasting Service Upgrades. *J. Mar. Sci. Eng.* **2022**, *10*, 149. [\[CrossRef\]](#)
35. Sotillo, M.G.; Cailleau, S.; Lorente, P.; Levier, B.; Aznar, R.; Reffray, G.; Amo-Baladrón, A.; Chanut, J.; Benkiran, M.; Fanjul, E.A. The MyOcean IBI Ocean Forecast and Reanalysis Systems: Operational Products and Roadmap to the Future Copernicus Service. *J. Oper. Oceanogr.* **2015**, *8*, 63–79. [\[CrossRef\]](#)
36. Fanjul, E.A.; Sotillo, M.G.; Pérez Gómez, B.; Garcia Valdecasas, J.M.; Perez Rubio, S.; Lorente, P.; Rodriguez Dapena, A.; Martinez Marco, I.; Luna, Y.; Padorno, E.; et al. Operational Oceanography at the Service of the Ports. *New Front. Oper. Oceanogr.* **2018**, *10*, 729–736.

37. Sotillo, M.G.; Mourre, B.; Mestres, M.; Lorente, P.; Aznar, R.; García-León, M.; Liste, M.; Santana, A.; Espino, M.; Álvarez, E. Evaluation of the Operational CMEMS and Coastal Downstream Ocean Forecasting Services During the Storm Gloria (January 2020). *Front. Mar. Sci.* **2021**, *8*, 644525. [CrossRef]
38. Willmott, C.J.; Robeson, S.M.; Matsuura, K. A Refined Index of Model Performance. *Int. J. Climatol.* **2012**, *32*, 2088–2094. [CrossRef]
39. Peters, H. Observations of Stratified Turbulent Mixing in an Estuary: Neap-to-Spring Variations During High River Flow. *Estuar. Coast. Shelf Sci.* **1997**, *45*, 69–88. [CrossRef]
40. Okubo, A. Oceanic Diffusion Diagrams. *Deep Sea Res. Oceanogr. Abstr.* **1971**, *18*, 789–802. [CrossRef]
41. Liu, Y.; Weisberg, R.H. Evaluation of Trajectory Modeling in Different Dynamic Regions Using Normalized Cumulative Lagrangian Separation. *J. Geophys. Res.* **2011**, *116*, C09013. [CrossRef]
42. Castro-Rosero, L.M.; Hernández, I.; Alsina, J.M.; Espino, M. Transport and Accumulation of Floating Marine Litter in the Black Sea: Insights from Numerical Modeling. *Front. Mar. Sci.* **2023**, *10*, 1213333. [CrossRef]
43. Révelard, A.; Reyes, E.; Mourre, B.; Hernández-Carrasco, I.; Rubio, A.; Lorente, P.; Fernández, C.D.L.; Mader, J.; Álvarez-Fanjul, E.; Tintoré, J. Sensitivity of Skill Score Metric to Validate Lagrangian Simulations in Coastal Areas: Recommendations for Search and Rescue Applications. *Front. Mar. Sci.* **2021**, *8*, 630388. [CrossRef]
44. Geopy: Python Geocoding Toolbox 2022. Available online: <https://pypi.org/project/geopy/> (accessed on 15 February 2024).
45. Jouon, A.; Douillet, P.; Ouillon, S.; Fraunié, P. Calculations of Hydrodynamic Time Parameters in a Semi-Opened Coastal Zone Using a 3D Hydrodynamic Model. *Cont. Shelf Res.* **2006**, *26*, 1395–1415. [CrossRef]
46. Riddle, A.M.; Lewis, R.E. Dispersion Experiments in U.K. Coastal Waters. *Estuar. Coast. Shelf Sci.* **2000**, *51*, 243–254. [CrossRef]
47. Shapely: Manipulation and Analysis of Geometric Objects 2024. Available online: <https://github.com/kannes/Shapely> (accessed on 20 February 2024).
48. Autoridad Portuaria de Gijón Memoria Anual Puerto Gijón 2022. 2022. Available online: https://www.puertogijon.es/wp-content/uploads/2023/11/memoria_apg_2022.pdf (accessed on 10 February 2024).
49. Simpson, J.H.; Brown, J.; Matthews, J.; Allen, G. Tidal Straining, Density Currents, and Stirring in the Control of Estuarine Stratification. *Estuaries* **1990**, *13*, 125. [CrossRef]
50. Alvarez, I.; Gomez-Gesteira, M.; deCastro, M.; Dias, J.M. Spatiotemporal Evolution of Upwelling Regime along the Western Coast of the Iberian Peninsula. *J. Geophys. Res.* **2008**, *113*, 2008JC004744. [CrossRef]
51. Díez-Minguito, M.; Baquerizo, A.; Ortega-Sánchez, M.; Navarro, G.; Losada, M.A. Tide Transformation in the Guadalquivir Estuary (SW Spain) and Process-based Zonation. *J. Geophys. Res.* **2012**, *117*, 2011JC007344. [CrossRef]
52. Cucco, A.; Umgiesser, G.; Ferrarin, C.; Perilli, A.; Canu, D.M.; Solidoro, C. Eulerian and Lagrangian Transport Time Scales of a Tidal Active Coastal Basin. *Ecol. Model.* **2009**, *220*, 913–922. [CrossRef]
53. Viero, D.P.; Defina, A. Water Age, Exposure Time, and Local Flushing Time in Semi-Enclosed, Tidal Basins with Negligible Freshwater Inflow. *J. Mar. Syst.* **2016**, *156*, 16–29. [CrossRef]
54. Carballo, R.; Iglesias, G.; Castro, A. Residual Circulation in the Ría de Muros (NW Spain): A 3D Numerical Model Study. *J. Mar. Syst.* **2009**, *75*, 116–130. [CrossRef]

Disclaimer/Publisher’s Note: The statements, opinions and data contained in all publications are solely those of the individual author(s) and contributor(s) and not of MDPI and/or the editor(s). MDPI and/or the editor(s) disclaim responsibility for any injury to people or property resulting from any ideas, methods, instructions or products referred to in the content.